NASA Contractor Report 165640

STRESS INTENSITY FACTORS IN A HOLLOW CYLINDER CONTAINING A RADIAL CRACK

F. Delale and F. Erdogan

LEHIGH UNIVERSITY
Bethlehem, Pennsylvania 18015

NASA Grant NGR 39-007-011
November 1980

National Aeronautics and
Space Administration

Langley Research Center
Hampton, Virginia 23665

STRESS INTENSITY FACTORS IN A HOLLOW CYLINDER CONTAINING A RADIAL CRACK*

by

F. Delale and F. Erdogan
Lehigh University, Bethlehem, Pa. 18015

Abstract

In this paper an exact formulation of the plane elasticity problem for a hollow cylinder or a disk containing a radial crack is given. The crack may be an external edge crack, an internal edge crack, or an embedded crack. It is assumed that on the crack surfaces the shear traction is zero and the normal traction is an arbitrary function of r. For various crack geometries and radius ratios, the numerical results are obtained for a uniform crack surface pressure, for a uniform pressure acting on the inside wall of the cylinder, and for a rotating disk.

1. Introduction

In this paper we reconsider the plane problem of a hollow cylinder containing an arbitrarily oriented radial crack and subjected to arbitrary normal tractions on the crack surfaces. Aside from its direct applications to plane problems such as cracked rings and rotating disks, the problem has potentially important applications to pressure vessels and piping containing a relatively long part-through crack in a meridional plane. In this latter group of three dimensional problems the plane strain solution provides an upper bound for the stress intensity factor in the mid-region of the longitudinal part-through crack in the cylinder wall. Because of the importance of the crack geometry, the problem has been studied rather extensively (see, for example, [1-7]). After Bueckner's early work in which the technique of complex potentials was used [1], most of the subsequent analytical studies were based on the

(*) This work was supported by the Department of Transportation under the Contract DOT-RC-82007, by NASA-Langley under the Grant NGR-007-011, and by NSF under the Grant ENG. 78-09737.

mapping technique originally developed by Bowie [2-4]. In [1] the problem of a rotating disk having a radial edge crack on its inner boundary is considered. The same crack geometry under uniform tensile tractions applied to the outer boundary of the ring is studied in [2]. The problem of multiple cracks located on the inner or outer boundary of the ring is considered in [3]. The problem of a curved beam or a ring segment containing a radial crack is studied in [4]. In [5] the problem of a hollow cylinder containing an external edge crack is considered for various loading conditions where a numerical technique similar to finite difference approximations is used for the solution. In [6] the ring problem with an inner edge crack is solved by using the method of weight functions. Needless to say, because of its plane geometry the problem is also ideally suited for a finite element treatment (see, for example, [7]).

There are, however, still sufficient reasons for reconsidering the problem. First, it may be observed that the existing solutions in one form or another are all restricted with regard to loading and/or geometry. Secondly, the published results are not, in most cases, sufficiently accurate in their entire domain of coverage. Third, it is desirable to have an exact analytical formulation and a reasonably simple and reliable method of solution for the problem which can be used by other investigators to obtain results to any desired degree of accuracy for particular crack geometries and loading conditions. Finally, the embedded crack problem has not been considered in any of the previous studies. In addition to its direct application to such problems as radial weld defects in longitudinal seams, the solution may be important in studying the crack problem in cylinders under self-equilibrating residual stresses (e.g., hollow tempered glass cylinders undergoing "static fatigue").

In this paper we consider the plane strain or the generalized plane stress problem for a concentric circular cylinder or ring containing a radial crack. It is assumed that the external loads are symmetric with respect to the plane of the crack and the basic ring problem without

the crack has been solved. Thus the main problem of interest is the Mode I crack problem in which the self-equilibrating arbitrary normal crack surface tractions are the only external loads (Figure 1a).

It should be pointed out that in the special cases of solid disk (Figure 1a, $a=0$, $b<\infty$) and the infinite plane with a circular hole ($0<a<\infty$, $b=\infty$), the problem may readily be formulated in terms of a singular integral equation by using the basic dislocation solutions given in [8] as the Green's functions.

2. Formulation of the Problem

The geometry and loading for the problem under consideration is shown in Figure 1a. In crack problems involving finite geometries, almost invariably the basic technique to formulate the problem is to express the solution as the sum of certain number of suitable solutions satisfying the differential equations of the problem in such a way that at least one of the solutions contains the main features of the general crack problem and the total solution contains sufficient number of arbitrary functions or sets of arbitrary constants to account for all boundary conditions. In this problem the solution is expressed as the sum of a crack or dislocation solution for an infinite plane and the general solution for a circular ring. In order to facilitate the application of the boundary conditions, the dislocation solution is expressed in polar rather than in rectangular coordinates. Let, then, the stress state in the cracked ring problem be of the following form:

$$\sigma_{ij}(r,\theta) = \sigma_{1ij}(r,\theta) + \sigma_{2ij}(r,\theta), \quad (i,j = r,\theta) \tag{1}$$

where σ_{1ij} and σ_{2ij}, $(i,j = r,\theta)$ respectively refer to an infinite plane containing an edge dislocation or a crack along $\theta=0$ line and to a concentric circular cylinder.

a) The infinite plane solution.

Consider an infinite plane with an edge dislocation having a Burger's vector $b_y = -f$ located at the point $r=t$, $\theta=0$ (Figure 1b). The plane

elasticity problem may be solved by assuming that

$$\sigma_{1r\theta} = 0,\ 0 \leq r < \infty,\ \theta = 0,\ \theta = \pi \tag{2}$$

$$\frac{\partial}{\partial r}\left[u_{1\theta}(r,+0) - u_{1\theta}(r,-0)\right] = f\delta(r-t),\ 0 \leq r < \infty. \tag{3}$$

Referring to [8] the Airy stress function of the problem may be expressed as (Figure 1b)

$$\psi_1(r,\theta) = -\frac{2\mu}{\pi(1+\kappa)} f\, r_1 \log r_1 \cos\theta_1$$

$$= -\frac{\mu}{\pi(1+\kappa)} f(r\cos\theta - t) \log (r^2+t^2-2rt\cos\theta), \tag{4}$$

where μ is the shear modulus, $\kappa=3-4\nu$ for plane strain and $\kappa= (3-\nu)/(1+\nu)$ for the generalized plane stress, ν being the Poisson's ratio. From (4) the stresses are obtained to be

$$\sigma_{1rr}(r,\theta) = \frac{1}{r}\frac{\partial\psi_1}{\partial r} + \frac{1}{r^2}\frac{\partial^2\psi_1}{\partial\theta^2}$$

$$= -\frac{2\mu f}{\pi(\kappa+1)}\left[\frac{r\cos\theta - t - 2t\sin^2\theta}{r^2+t^2 - 2rt\cos\theta}\right.$$

$$\left. - \frac{2t^2\sin^2\theta(r\cos\theta - t)}{(r^2+t^2 - 2rt\cos\theta)^2}\right], \tag{5}$$

$$\sigma_{1r\theta}(r,\theta) = -\frac{\partial}{\partial r}\left(\frac{1}{r}\frac{\partial\psi_1}{\partial\theta}\right)$$

$$= \frac{2\mu f}{\pi(\kappa+1)}\left[\frac{\sin\theta(2t\cos\theta - r)}{r^2+t^2 - 2rt\cos\theta}\right.$$

$$\left. - \frac{2t\sin\theta(r\cos\theta - t)(r - t\cos\theta)}{(r^2+t^2 - 2rt\cos\theta)^2}\right], \tag{6}$$

$$\sigma_{1\theta\theta}(r,\theta) = \frac{\partial^2\psi_1}{\partial r^2}$$

$$= -\frac{2\mu f}{\pi(\kappa+1)}\left[\frac{2\cos\theta(r - t\cos\theta) + r\cos\theta - t}{r^2+t^2 - 2rt\cos\theta}\right.$$

$$\left. - \frac{2(r\cos\theta - t)(r - t\cos\theta)^2}{(r^2+t^2 - 2rt\cos\theta)^2}\right]. \tag{7}$$

With an eye on combining the infinite plane solution with the ring solution, we now express the normal and shear components of the stress state along the circles r=a and r=b in the plane in terms of the following Fourier series:

$$\sigma_{1r\theta}(a,\theta) = \frac{\mu f}{\pi(1+\kappa)} \sum_{1}^{\infty} A_n(t) \sin n\theta, \tag{8}$$

$$\sigma_{1rr}(a,\theta) = -\frac{\mu f}{\pi(1+\kappa)} \sum_{0}^{\infty} B_n(t) \cos n\theta, \tag{9}$$

$$\sigma_{1r\theta}(b,\theta) = \frac{\mu f}{\pi(1+\kappa)} \sum_{1}^{\infty} C_n(t) \sin n\theta, \tag{10}$$

$$\sigma_{1rr}(b,\theta) = -\frac{\mu f}{\pi(1+\kappa)} \sum_{0}^{\infty} D_n(t) \cos n\theta, \tag{11}$$

where the Fourier coefficients are given by

$$A_n(t) = \frac{2}{\pi} \int_0^{\pi} \left[\frac{2 \sin\theta(2t\cos\theta - a)}{a^2+t^2 - 2at\cos\theta} - \frac{4t \sin\theta(a\cos\theta - t)(a - t\cos\theta)}{(a^2+t^2 - 2at\cos\theta)^2} \right] \sin n\theta \, d\theta, \tag{12}$$

$$B_0(t) = \left(-\frac{\pi(1+\kappa)}{\mu f}\right) \frac{1}{\pi} \int_0^{\pi} \sigma_{1rr}(a,\theta) d\theta,$$

$$B_n(t) = \left(-\frac{\pi(1+\kappa)}{\mu f}\right) \frac{2}{\pi} \int_0^{\pi} \sigma_{1rr}(a,\theta) \cos n\theta \, d\theta; \tag{13a,b}$$

$$C_n(t) = \left(\frac{\pi(1+\kappa)}{\mu f}\right) \frac{2}{\pi} \int_0^{\pi} \sigma_{1r\theta}(b,\theta) \sin n\theta \, d\theta, \tag{14}$$

$$D_0(t) = \left(1 \frac{\pi(1+\kappa)}{\mu f}\right) \frac{1}{\pi} \int_0^{\pi} \sigma_{1rr}(b,\theta) d\theta,$$

$$D_n(t) = \left(-\frac{\pi(1+\kappa)}{\mu f}\right) \frac{2}{\pi} \int_0^{\pi} \sigma_{1rr}(b,\theta) \cos n\theta \, d\theta \tag{15a,b}$$

After some manipulations and combining some of the terms, the integrals which appear in (12-15) can be evaluated in closed form, giving

$$A_n(t) = \frac{1}{a}\left\{\frac{a^2}{t^2-a^2}\left[n\left(\frac{a}{t}\right)^{n+1} - (n-4)\left(\frac{a}{t}\right)^{n-3}\right] + 2n\left(\frac{a}{t}\right)^{n+1}\right.$$

$$\left. - \frac{2a^4}{(t^2-a^2)^2}\left[\left(\frac{a}{t}\right)^{n-5} - \left(\frac{a}{t}\right)^{n-1}\right]\right\}, \quad n \geq 2, \tag{16}$$

$$B_0(t) = -\frac{2}{t},$$

$$B_n(t) = \frac{1}{a}\left\{\frac{4a^4}{(t^2-a^2)^2}\left[\left(\frac{a}{t}\right)^{n-3} - \frac{1}{2}\left(\frac{a}{t}\right)^{n-1} - \frac{1}{2}\left(\frac{a}{t}\right)^{|n-2|-3}\right]\right.$$

$$+ 2\left(\frac{a}{t}\right)^{n+1}\frac{t^2+a^2}{t^2-a^2} - \frac{a^2}{t^2-a^2}\left[n\left(\frac{a}{t}\right)^{n+1}\right.$$

$$\left.\left. -(2n-8)\left(\frac{a}{t}\right)^{n-1} + (|n-2|-2)\left(\frac{a}{t}\right)^{|n-2|-1}\right]\right\}, \quad n \geq 1, \tag{17a,b}$$

$$C_n(t) = \frac{1}{b}\left\{\frac{2b^4}{(b^2-t^2)^2}\left[\left(\frac{t}{b}\right)^{n+1} - \left(\frac{t}{b}\right)^{n+5}\right] - 2n\left(\frac{t}{b}\right)^{n-1}\right.$$

$$\left. + \frac{b^2}{b^2-t^2}\left[n\left(\frac{t}{b}\right)^{n-1} - (n+4)\left(\frac{t}{b}\right)^{n+3}\right]\right\}, \quad n \geq 2, \tag{18}$$

$$D_0(t) = -\frac{2t}{b^2},$$

$$D_n(t) = \frac{1}{b}\left\{-\frac{2b^2}{b^2-t^2}\left[(n+3)\left(\frac{t}{b}\right)^{n+1} - \frac{n+4}{2}\left(\frac{t}{b}\right)^{n+3}\right.\right.$$

$$\left. - \frac{1}{2}(|n-2|+2)\left(\frac{t}{b}\right)^{|n-2|+1}\right] + \frac{2b^2}{b^2-t^2}\left(\frac{t}{b}\right)^{n-1}$$

$$\left. - \frac{4b^4}{(b^2-t^2)^2}\left[\left(\frac{t}{b}\right)^{n+3} - \frac{1}{2}\left(\frac{t}{b}\right)^{n+5} - \frac{1}{2}\left(\frac{t}{b}\right)^{|n-2|+3}\right]\right\}, \quad n \geq 1, \tag{19a,b}$$

b) *The ring solution.*

In this case assuming a stress function of the form

$$\psi_2(r,\theta) = F(r)e^{\beta\theta} \tag{20}$$

the general elasticity solution in polar coordinates may be obtained as [9]

$$\psi_2(r,\theta) = a_0 + b_0 \log r + c_0 r^2 + d_0 r^2 \log r$$

$$+ (a_0' + b_0' \log r + c_0' r^2 + d_0' r^2 \log r)\theta$$

$$+ (a_1 r + b_1 r \log r + \frac{c_1}{r} + d_1 r^3) \begin{matrix}\sin\theta \\ \cos\theta\end{matrix}$$

$$+ (a_1' r + b_1' r \log r)\theta \begin{matrix}\sin\theta \\ \cos\theta\end{matrix}$$

$$+ \sum_{n=2}^{\infty} (a_n r^n + b_n r^{n+2} + c_n r^{-n} + d_n r^{2-n}) \begin{matrix}\sin n\theta \\ \cos n\theta\end{matrix} . \qquad (21)$$

This is basically the solution given by Michell, except that he omitted some of the repeated roots. From (21) the stresses for an annulus are found to be

$$\sigma_{2rr} = \frac{b_0}{r^2} + 2c_0 + (-\frac{2c_1}{r^3} + 2d_1 r) \begin{matrix}\sin\theta \\ \cos\theta\end{matrix}$$

$$- \frac{3+\nu}{4\pi r} (R_y \sin\theta + R_x \cos\theta) - \sum_{n=2}^{\infty} [a_n n(n-1) r^{n-2}$$

$$+ b_n (n+1)(n-2) r^n + c_n n(n+1) r^{-(n+2)} + d_n (n-1)(n+2) r^{-n}] \begin{matrix}\sin n\theta \\ \cos n\theta\end{matrix} ,$$

$$\sigma_{2\theta\theta} = - \frac{b_0}{r^2} + 2c_0 + (\frac{2c_1}{r^3} + 6d_1 r) \begin{matrix}\sin\theta \\ \cos\theta\end{matrix} + \frac{1-\nu}{4\pi r} (R_y \sin\theta + R_x \cos\theta)$$

$$+ \sum_{n=2}^{\infty} [a_n n(n-1) r^{n-2} + b_n (n+1)(n+2) r^n$$

$$+ c_n n(n+1) r^{-(n+2)} + d_n (n-2)(n-1) r^{-n}] \begin{matrix}\sin n\theta \\ \cos n\theta\end{matrix} ,$$

$$\sigma_{2r\theta} = \frac{a_0'}{r^2} + \left(\frac{2c_1}{r^3} - 2d_1 r\right)\begin{matrix}\cos\theta \\ -\sin\theta\end{matrix} - \frac{1-\nu}{4\pi r}\left(R_y\cos\theta + R_x\sin\theta\right)$$

$$- \sum_{n=2}^{\infty} \left[a_n n(n-1)r^{n-2} + b_n n(n+1)r^n - c_n n(n+1)r^{-(n+2)}\right.$$

$$\left. - d_n n(n-1)r^{-n}\right]\begin{matrix}\cos n\theta \\ -\sin n\theta\end{matrix}, \qquad (22a\text{-}c)$$

where R_x and R_y are the resultants of the tractions on r=a. In the problem under consideration $R_x=0$, $R_y=0$ and the stresses satisfy the following symmetry conditions:

$$\sigma_{2rr}(r,\theta) = \sigma_{2rr}(r,-\theta),\ \sigma_{2\theta\theta}(r,\theta) = \sigma_{2\theta\theta}(r,-\theta),$$

$$\sigma_{2r\theta}(r,\theta) = -\sigma_{2r\theta}(r,-\theta). \qquad (23a\text{-}c)$$

Thus, from (22) and (23) it follows that

$$\sigma_{2rr} = \frac{b_0}{r^2} + 2c_0 + \left(-\frac{2c_1}{r^3} + 2d_1 r\right)\cos\theta - \sum_{2}^{\infty} \left[a_n n(n-1)r^{n-2}\right.$$

$$\left. + b_n(n+1)(n-2)r^n + c_n n(n+1)r^{-n-2} + d_n(n-1)(n+2)r^{-n}\right]\cos n\theta,$$

$$\sigma_{2r\theta} = \left(-\frac{2c_1}{r^3} + 2d_1 r\right)\sin\theta + \sum_{2}^{\infty} \left[a_n n(n-1)r^{n-2}\right.$$

$$\left. + b_n n(n+1)r^n - c_n n(n+1)r^{-n-2} - d_n n(n-1)r^{-n}\right]\sin n\theta,$$

$$\sigma_{2\theta\theta} = -\frac{b_0}{r^2} + 2c_0 + \left(\frac{2c_1}{r^3} + 6d_1 r\right)\cos\theta + \sum_{2}^{\infty} \left[a_n n(n-1)r^{n-2}\right.$$

$$\left. + b_n(n+1)(n+2)r^n + c_n n(n+1)r^{-n-2} + d_n(n-2)(n-1)r^{-n}\right]\cos n\theta .$$

$$(24a\text{-}c)$$

c) *Boundary conditions.*

After determining the basic form of the solutions for the infinite plate with a dislocation and for the ring, the stresses in the ring

having a dislocation may be expressed as the sum of the two solutions (see (1), (5-7) and (24)). The combined stress state must then satisfy the following boundary conditions (Figure 1a):

$$\sigma_{1rr}(a,\theta) + \sigma_{2rr}(a,\theta) = 0,\ 0 \le \theta \le \pi ,$$

$$\sigma_{1r\theta}(a,\theta) + \sigma_{2r\theta}(a,\theta) = 0,\ 0 \le \theta \le \pi ,$$

$$\sigma_{1rr}(b,\theta) + \sigma_{2rr}(b,\theta) = 0,\ 0 \le \theta \le \pi ,$$

$$\sigma_{1r\theta}(b,\theta) + \sigma_{2r\theta}(b,\theta) = 0,\ 0 \le \theta \le \pi \qquad (25\ a\text{-}d)$$

$$\sigma_{1\theta\theta}(r,0) + \sigma_{2\theta\theta}(r,0) = g(r),\ c < r < d \qquad (26)$$

where σ_{1rr} and $\sigma_{1r\theta}$ are given by (8-15) and σ_{2rr} and $\sigma_{2r\theta}$ are given by (24), and $g(r)$ is the crack surface traction. Note that each equation in (25) is a sine or cosine series in which the coefficients of $\sin n\theta$ and $\cos n\theta$, $(n=0,1,\ldots)$ must vanish. Thus, defining

$$a_n = -\frac{\mu f}{\pi(\kappa+1)}\alpha_n ,\ b_n = -\frac{\mu f}{\pi(\kappa+1)}\beta_n ,$$

$$c_n = -\frac{\mu f}{\pi(\kappa+1)}\gamma_n ,\ d_n = -\frac{\mu f}{\pi(\kappa+1)}\delta_n ,\ (n=0,1,\ldots) , \qquad (27\ a\text{-}d)$$

we obtain

$$\frac{\beta_o}{a^2} + 2\gamma_o = -B_o ,\ \frac{\beta_o}{b^2} + 2\gamma_o = -D_o ; \qquad (28a,b)$$

$$-\frac{2\gamma_1}{a^3} + 2\delta_1 a = -B_1 ,\ -\frac{2\gamma_1}{a^3} + 2\delta_1 b = -D_1 ; \qquad (29a,b)$$

$$-\frac{2\gamma_1}{a^3} + 2\delta_1 a = A_1 ,\ -\frac{2\gamma_1}{a^3} + 2\delta_1 b = C_1 ; \qquad (30a,b)$$

$$\alpha_n\, n(n-1)a^{n-2} + \beta_n(n+1)(n-2)a^{n} + \gamma_n\, n(n+1)a^{-n-2}$$

$$+ \delta_n(n-1)(n+2)a^{-n} = B_n\ ,\ (n=2,3,\ldots)\ ,$$

$$\alpha_n\, n(n-1)a^{n-2} + \beta_n\, n(n+1)a^{n} - \gamma_n\, n(n+1)a^{-n-2}$$

$$- \delta_n\, n(n-1)a^{-n} = A_n\ ,\ (n=2,3,\ldots)\ ,$$

$$\alpha_n\, n(n-1)b^{n-2} + \beta_n(n+1)(n-2)b^{n} + \gamma_n\, n(n+1)b^{-n-2}$$

$$+ \delta_n(n-1)(n+2)b^{-n} = D_n,\ (n=2,3,\ldots),$$

$$\alpha_n\, n(n-1)b^{n-2} + \beta_n\, n(n+1)b^{n} - \gamma_n\, n(n+1)b^{-n-2}$$

$$- \delta_n\, n(n-1)b^{-n} = C_n\ ,\ (n=2,3,\ldots)\ , \qquad (31a\text{-}d)$$

where A_n, B_n, C_n, and D_n, (n=0,1,2,...) are known functions of t and are given by (16-19). Consequently, the coefficients a_n, b_n, c_n, and d_n calculated from (27-31) will also be functions of t. From (24) it may be observed that the coefficients a_0, a_1, b_1 and d_0 do not appear in the expressions of σ_{2ij}. Therefore, if the series in (24) are truncated at the nth term, there would be 4n unknown coefficients to be determined. On the other hand, there are 4n+2 equations in the corresponding algebraic system given by (28-31). Two of these equations must, therefore, be redundant. This is, in fact, suggested by the pairs of equations (29a, 30a) and (29b, 30b). These equations indicate that if

$$A_1 + B_1 = 0\ ,\ C_1 + D_1 = 0\ , \qquad (32a,b)$$

then (29) and (30) are identical and by, for example, ignoring (30), the unknown coefficients may be determined uniquely from (28), (29), and (31). Referring to (8) and (9), it may be seen that

$$A_1 + B_1 = \frac{\pi(1+\kappa)}{\mu f}\frac{1}{\pi a}\int_0^{2\pi}[\sigma_{1r\theta}(a,\theta)\sin\theta - \sigma_{1rr}(a,\theta)\cos\theta]ad\theta. \tag{33}$$

Consider now an infinite plane containing an edge dislocation at x=t (see eqs. (2,3)). If we introduce a circular hole r=a, a<t into the plane (Fig. 1), then certain tractions σ_{1rr} and $\sigma_{1r\theta}$ must be applied along the boundary of the hole in order to maintain the equilibrium of the plane. It is clear that the integral in (33) is nothing but the x-component of the resultant of these tractions. Since the external force system due to the dislocation or the crack (which results from (2) and (3)) is self-equilibrating, this resultant must be zero, proving the validity of (32a). Equation (32b) follows from similar arguments for a disk $r\leq b$ containing a dislocation at x=t<b. It is because of the relations (32) that in (16-19) the expressions for A_1 and C_1 are not included.

After expressing the coefficients $a_n,\ldots,d_n$ in terms of f, the remaining boundary condition (26) may be used to determine f. If we now assume that the crack is formed by distributing the dislocations along the line θ=0, c<r<d with f as a function of t, $\sigma_{\theta\theta}(r,\theta)$ in the ring may be evaluated by integrating the Green's function obtained from (1), (7), (24c) and (27-32). Specifically, for θ=0 from (26) we find

$$\int_c^d \frac{f(t)}{t-r}dt + \int_c^d k(r,t)f(t)dt = \frac{\pi(\kappa+1)}{2\mu}g(r),\quad c<r<d, \tag{34}$$

where

$$k(r,t) = -\frac{1}{2}\{-\frac{\beta_0}{r^2} + 2\gamma_0 + \frac{2\gamma_1}{r^3} + 6\delta_1 r + \sum_2^\infty [n(n-1)\alpha_n r^{n-2} + (n+1)(n+2)\beta_n r^n + n(n+1)\gamma_n r^{-n-2} + (n-2)(n-1)\delta_n r^{-n}], \tag{35}$$

and α_n, β_n, γ_n, and δ_n (n=0,1,...) are known functions of t which are determined from (28-32). If the crack is an embedded crack (i.e., if a<c<d<b) then from the definition of f(t) given by (3) it follows that

$$\int_c^d f(t)dt = 0 \quad . \tag{36}$$

3. Stress Intensity Factors and Examples

If the crack is an embedded crack, the index of the integral equation (34) is +1 and the solution is of the following form

$$f(r) = \frac{F(r)}{[(r-c)(d-r)]^{\frac{1}{2}}} \ , \ (c<r<d) \tag{37}$$

where F(r) is a bounded function. After evaluating F(r), the stress intensity factors at the crack tips r=c and r=d may be defined and obtained from

$$k(c) = \lim_{r\to c} \sqrt{2(c-r)}\ \sigma_{\theta\theta}\ (r,0)$$

$$= \frac{2\mu}{1+\kappa} \lim_{r\to c} \sqrt{2(r-c)}\ f(r) = \frac{2\mu}{1+\kappa} \frac{F(c)}{\sqrt{(d-c)/2}} \ , \tag{38}$$

$$k(d) = \lim_{r\to d} \sqrt{2(r-d)}\ \sigma_{\theta\theta}(r,0)$$

$$= -\frac{2\mu}{1+\kappa} \lim_{r\to d} \sqrt{2(d-r)}\ f(r) = -\frac{2\mu}{1+\kappa} \frac{F(d)}{\sqrt{(d-c)/2}} \quad . \tag{39}$$

The singular integral equation (34) may be solved numerically by normalizing the interval (c,d) to (-1,1) and by using the Gaussian integration formula [10]. Since the Fredholm kernel k(r,t) is given in a simple form, one could obtain the results to any desired degree of accuracy with a relatively modest computational effort.

In the case of an edge crack (i.e., for a=c<d<b or a<c<d=b) the single-valuedness condition (36) is not valid and also is not required as an additional condition for a unique solution.

For certain ring-crack geometries the convergence of the infinite series giving the Fredholm kernel (35) was rather slow. The results given in this paper were obtained by truncating the series at the Nth term, solving the integral equations for N=100, 120, and 140 for each ring-crack geometry and loading condition considered, calculating the stress intensity factors k as a function of N (from (38) and (39)), and by using a curve-fitting procedure of the following form

$$k(N_i) = A + \frac{B}{N_i^{\alpha}} , \quad (N_1 = 100,\ N_2 = 120,\ N_3 = 140) . \tag{40}$$

The value of A obtained from (40) is assumed to be the calculated stress intensity factor. In the examples, for the values N_i considered, α is generally greater than unity, implying that the slope of k vs. 1/N curve at (1/N) = 0 is zero. Also, since the values $k(N_i)$ (i=1,2,3) differ from each other only in the third or fourth significant digits in the slowest converging cases, the extrapolated values ought to be quite reliable.

Three different loading conditions are used in the examples. Note that g(r) which appear as the input function in the integral equation (34) or as the traction in the boundary condition (26) is the value of $\sigma_{\theta\theta}$ in the perturbation problem. For the loading conditions considered, g(r) is given by the following expressions:

a) Uniform crack surface pressure

$$g(r) = -\sigma_0 , \quad c < r < d. \tag{41}$$

b) Internally pressurized cylinder

$$g(r) = -\frac{p_0 a^2}{b^2 - a^2}\left(1 + \frac{b^2}{r^2}\right) , \quad c < r < d , \tag{42}$$

where p_0 is the internal pressure (i.e., $\sigma_{rr}(a,\theta) = -p_0$). Here, it should be observed that in the case of the internal edge crack (i.e.,

for $c = a < d < b$), in addition to $g(r)$ given by (42), the crack surfaces may be subjected to uniform (fluid) pressure $g(r) = -p_o$. If that is the case, then the stress intensity factor separately obtained from $g(r) = -p_o$ should be added to that given by (42). In the examples, results due to (41) and (42) are listed separately.

c) *Rotating disk*

$$g(r) = -\frac{3+\nu}{8}\rho\,\omega^2\left[a^2 + b^2 + \left(\frac{ab}{r}\right)^2 - \frac{1+3\nu}{3+\nu}r^2\right] \qquad (43)$$

where ρ is the mass density and ω is the angular velocity. The expression given in (43) is for the generalized plane stress and is valid for a rotating "disk". For a long rotating hollow cylinder, i.e., for the plane strain case, we have

$$g(r) = -\frac{1}{8}\frac{3-2\nu}{1-\nu}\rho\,\omega^2\left[b^2 + a^2 + \left(\frac{ab}{r}\right)^2 - \frac{1+2\nu}{3-2\nu}r^2\right]. \qquad (44)$$

For various crack geometries the calculated stress intensity factors are shown in Tables 1-8. To give some idea about the trends, some limited results are also given in Figures 2-5. Table 1 gives the results for an embedded crack symmetrically located with respect to the boundaries of the ring or the hollow cylinder and subjected to a uniform crack surface pressure (see (41)). Here the crack length is fixed at half the wall thickness b-a and the ratio of a/b is varied. The results are also displayed in Figure 2. Intuitively, it may be argued that the "constraint" at the inner crack tip r=c is greater and at the outer crack tip r=d is less than that of a centrally cracked infinite strip. Therefore, one may expect that k(c) should be less and k(d) should be greater than the corresponding stress intensity factor in the strip. This trend may also be observed in Figure 2 where the ring results seem to approach the strip value as $a\to\infty$ for constant wall thickness b-a.

Table 2 shows the effect of the crack length on the stress intensity factors in a ring or a hollow cylinder with a fixed radius ratio

Table 1. Stress intensity factors k(c) and k(d) for an embedded crack in a ring or a hollow cylinder subjected to uniform crack surface pressure $\sigma_{\theta\theta}(r,0) = -\sigma_o$. $\frac{d-c}{b-a} = 0.5$, $\frac{c-a}{b-d} = 1$ (Figure 1a)

$\frac{a}{b-a}$	$\frac{k(c)}{\sigma_o\sqrt{(d-c)/2}}$	$\frac{k(d)}{\sigma_o\sqrt{(d-c)/2}}$
0.05	1.1477	1.2046
0.10	1.1498	1.2030
0.25	1.1580	1.2018
0.50	1.1664	1.2007
1.0	1.1736	1.1980
2.0	1.1788	1.1943
3.0	1.1810	1.1923
4.0	1.1822	1.1911
∞	1.1867	1.1867

Table 2. Stress intensity factors k(c) and k(d) for an embedded crack in a ring or a hollow cylinder subjected to uniform crack surface pressure $\sigma_{\theta\theta}(r,0) = -\sigma_o$ (columns 2 and 3) or internal pressure $\sigma_{rr}(a,\theta) = -p_o$ (columns 4 and 5). $\frac{a}{b} = \frac{1}{2}$, $\frac{c-a}{b-d} = 1$ (Figure 1a) (The last column refers to the centrally cracked infinite strip)

$\frac{d-c}{b-a}$	$\frac{k(c)}{\sigma_o\sqrt{(d-c)/2}}$	$\frac{k(d)}{\sigma_o\sqrt{(d-c)/2}}$	$\frac{k(c)}{p_o\sqrt{(d-c)/2}}$	$\frac{k(d)}{p_o\sqrt{(d-c)/2}}$	$\frac{k}{\sigma_o\sqrt{(d-c)/2}}$
→0.0	1.0	1.0	0.9259	0.9259	1.0
0.1	1.0060	1.0062	0.9522	0.9129	1.0060
0.2	1.0241	1.0256	0.9920	0.9139	1.0246
0.3	1.0556	1.0608	1.0468	0.9311	1.0577
0.4	1.1034	1.1158	1.1201	0.9682	1.1094
0.5	1.1736	1.1980	1.2186	1.0318	1.1867
0.6	1.2785	1.3213	1.3557	1.1341	1.3033
0.7	1.4445	1.5146	1.5606	1.3010	1.4884
0.8	1.7407	1.8536	1.9084	1.6002	1.8169
→1.0	∞	∞	∞	∞	∞

Table 3. Stress intensity factors k(c) and k(d) for an embedded crack in a ring or a hollow cylinder subjected to uniform crack surface pressure $\sigma_{\theta\theta}(r,0) = -\sigma_0$ (columns 2 and 3) or internal pressure $\sigma_{rr}(a,\theta) = -p_0$ (columns 4 and 5). $\frac{d-c}{b-a} = 0.5$, $\frac{a}{b} = \frac{1}{2}$ (Figure 1a)

$\frac{c-a}{b-a}$	$\frac{k(c)}{\sigma_0\sqrt{(d-c)/2}}$	$\frac{k(d)}{\sigma_0\sqrt{(d-c)/2}}$	$\frac{k(c)}{p_0\sqrt{(d-c)/2}}$	$\frac{k(d)}{p_0\sqrt{(d-c)/2}}$
0.15	1.2414	1.1755	1.4292	1.1004
0.20	1.1929	1.1777	1.3033	1.0554
0.25	1.1736	1.1980	1.2186	1.0318
0.30	1.1744	1.2391	1.1608	1.0290
0.35	1.1936	1.3118	1.1249	1.0533

a/b = 1/2. The crack is again symmetrically located with respect to the boundaries (i.e., c-a = b-d). The table shows the results for uniform crack surface pressure σ_0 (columns 2 and 3), for internal (wall) pressure p_0 (columns 4 and 5), and, for the purpose of comparison, for a centrally cracked infinite strip (column 6). Again to show the general trend of the results, the stress intensity factors for a cylinder under internal pressure p_0 are also displayed in Figure 3. In this case, as the crack length d-c goes to zero, the stress intensity factors k(c) and k(d) approach $\sigma_{\theta\theta}(\frac{a+b}{2}), 0)\sqrt{(d-e)/2}$ which is the corresponding infinite plane result (for a/b=1/2, $\sigma_{\theta\theta}(\frac{a+b}{2}, 0) = (25/27)\ p_0 \cong 0.9259\ p_0$). In this problem the initial decrease in k(d) with increasing crack length is due to the decrease in $\sigma_{\theta\theta}(r,0)$ in the neighborhood of r=d.

The effect of the relative position of the crack in the cylinder wall is shown in Table 3. Here it is assumed that the crack length and radius ratio of the cylinder are constant ((d-c) = (b-a)/2, a = b/2) and the radial position of the crack (c-a)/(b-a) is varied.

The results for an internal edge crack c = a<d<b are given in Tables 4-6. Table 4 shows the stress intensity factor for a uniform crack surface pressure σ_0 (see (41)). The strip results given in the last column of the table are the limit of the cylinder results for

Table 4. The normalized stress intensity factor $k(d)/(\sigma_o\sqrt{d-a})$ in a hollow cylinder or a ring containing an internal edge crack ($c=a<d<b$) and subjected to uniform crack surface pressure $\sigma_{\theta\theta}(r,0) = -\sigma_o$.

$\frac{d-a}{b-a}$ \ $\frac{a}{b-a}$	1/3	1/2	1	2	3	∞ (strip)
→0	1.1216	1.1216	1.1216	1.1216	1.1216	1.1216
0.1	1.153	1.155	1.157	1.159	1.167	1.1893
0.2	1.218	1.229	1.247	1.277	1.299	1.3674
0.3	1.295	1.310	1.366	1.449	1.493	1.6601
0.4	1.373	1.402	1.503	1.655	1.747	2.1119
0.5	1.465	1.508	1.658	1.901	2.066	2.8258
0.6	1.578	1.635	1.830	2.177	2.441	4.035
0.7	1.730	1.796	2.030	2.475	2.851	6.361
→1.0	∞	∞	∞	∞	∞	∞

Table 5. The normalized stress intensity factor $k(d)/[\sigma_{\theta\theta}(a,0)\sqrt{d-a}]$ for an internal edge crack ($c=a<d<b$) in a hollow cylinder under internal pressure, $\sigma_{rr}(a,\theta) = -p_o$. (The effect of pressure p on the crack surfaces are not included) $\sigma_{\theta\theta}(a,0) = p_o(b^2+a^2)/(b^2-a^2)$.

$\frac{d-a}{b-a}$ \ $\frac{a}{b-a}$	1/3	1/2	1	2	3
→0	1.1216	1.1216	1.1216	1.1216	1.1216
0.1	0.878	0.957	1.058	1.113	1.137
0.2	0.756	0.878	1.057	1.189	1.239
0.3	0.685	0.834	1.089	1.305	1.397
0.4	0.643	0.813	1.138	1.461	1.613
0.5	0.620	0.808	1.199	1.635	1.883
0.6	0.611	0.816	1.273	1.834	2.189
0.7	0.616	0.841	1.359	2.046	2.527
→1	∞	∞	∞	∞	∞

Table 6. The normalized stress intensity factor $k(d)/[\sigma_{\theta\theta}(a,0)\sqrt{d-a}]$ for an internal edge crack ($c=a<d<b$) in a rotating disk ($\nu=0.3$) $\sigma_{\theta\theta}(a,0) = \frac{3+\nu}{4}\ \rho\ \omega^2\ (b^2 + \frac{1-\nu}{3+\nu}\ a^2)$.

$\frac{d-a}{b-a}$ \ $\frac{a}{b-a}$	1/3	1/2	1	2	3
→0.0	1.1216	1.1216	1.1216	1.1216	1.1216
0.1	1.008	1.040	1.089	1.120	1.139
0.2	0.962	1.018	1.114	1.202	1.240
0.3	0.944	1.018	1.168	1.324	1.401
0.4	0.943	1.032	1.235	1.477	1.617
0.5	0.956	1.058	1.315	1.664	1.879
0.6	0.981	1.096	1.405	1.867	2.196
0.7	1.025	1.153	1.508	2.082	2.526
→1.0	∞	∞	∞	∞	∞

$a\to\infty$ and for constant wall thickness b-a. The results of Table 4 are partly displayed in Figure 4 to show the general trend. One may again note that as a/(b-a) increases, the geometric constraints decrease causing an increase in the stress intensity factors. As the crack length d-a tends to zero, the stress intensity factor ratio approaches that of a half plane with an edge crack namely, 1.1216.

Table 5 and Figure 5 show the stress intensity factor k(d) for a hollow cylinder with an internal edge crack and subjected to internal pressure $\sigma_{rr}(a,\theta) = -p_o$. Note that k(d) is normalized with respect to the hoop stress at the inner boundary of the cylinder, $\sigma_{\theta\theta}(a,\theta) = p_o(b^2+a^2)/(b^2-a^2)$. Figure 5 also shows the variation of the hoop stress $\sigma_{\theta\theta}(r,\theta)$ through the cylinder wall, again normalized with respect to $\sigma_{\theta\theta}(a,\theta)$. Thus, the initial decrease in k(d) for increasing crack length d-a in cylinders having small values of a/(b-a) may easily be explained by the relatively sharp decrease in $\sigma_{\theta\theta}(r,\theta)$ (which is the external load applied to the crack surface). Again, as $d-a\to 0$, the stress intensity

factor ratio tends to the half-plane value 1.1216.

The rotating disk or cylinder results are given in Table 6. Here, too, the stress intensity factor k(d) is normalized with respect to the hoop stress $\sigma_{\theta\theta}$ at the inner boundary r=a, the expression of which is given in the table (see (43)). Note that the expressions of the hoop stress $\sigma_{\theta\theta}$ in the rotating disk and in the long hollow cylinder are different and are dependent on the Poisson's ratio ν. Therefore, the problems for the disk and the cylinder must be solved separately for a specified value of ν. The results given in Tables 6 and 8 are for the rotating disk which are obtained by using the plane stress solution with ν=0.3.

The results for a hollow cylinder or a disk with an external edge crack are given in Tables 7 and 8. Table 7 shows the results for an internally pressurized hollow cylinder or disk. The stress intensity factor for a rotating disk obtained again from the plane stress solution with ν=0.3 is given in Table 8.

Table 7. The normalized stress intensity factor $k(c)/[\sigma_{\theta\theta}(b,0)\sqrt{b-c}]$ for an external edge crack (a<c<d=b) in a hollow cylinder or a disk under internal pressure $\sigma_{rr}(a,\theta) = -p_o$; $\sigma_{\theta\theta}(b,0) = 2a^2p_o/(b^2-a^2)$.

$\frac{b-c}{b-a}$ \ $\frac{a}{b-a}$	1/3	1/2	1	2	3
→0	1.1216	1.1216	1.1216	1.1216	1.1216
0.1	1.250	1.245	1.219	1.203	1.208
0.2	1.413	1.391	1.368	1.355	1.352
0.3	1.617	1.587	1.557	1.560	1.574
0.4	1.874	1.829	1.797	1.832	1.873
0.5	2.207	2.137	2.095	2.170	2.259
0.6	2.655	2.540	2.462	2.586	2.740
0.7	3.301	3.103	2.941	3.085	3.320
→1.0	→∞	→∞	→∞	→∞	→∞

Table 8. The normalized stress intensity factor $k(c)/(\sigma_{\theta\theta}(b,0)\sqrt{b-c})$ in a rotating disk having an external edge crack ($a<c<d=b$). $\sigma_{\theta\theta}(b,0) = \frac{3+\nu}{4}\ \rho\ \omega^2(a^2 + \frac{1-\nu}{3+\nu}\ b^2)$, $\nu = 0.3$.

$\frac{b-c}{b-a}$ \ $\frac{a}{b-a}$	1/3	1/2	1	2	3
→0	1.1216	1.1216	1.1216	1.1216	1.1216
0.1	1.312	1.288	1.245	1.217	1.214
0.2	1.530	1.486	1.419	1.377	1.367
0.3	1.774	1.714	1.632	1.608	1.601
0.4	2.053	1.982	1.893	1.894	1.911
0.5	2.380	2.299	2.210	2.242	2.309
0.6	2.777	2.691	2.601	2.682	2.811
0.7	3.301	3.210	3.093	3.199	3.406
→1.0	→∞	→∞	→∞	→∞	→∞

References

1. H.F. Bueckner and I. Giaever, "The stress concentration of a notched rotor subjected to centrifugal forces", ZAMM, Vol. 46, pp. 265-273, 1966.

2. O.L. Bowie and C.E. Freese, "Elastic analysis for a radial crack in a circular ring", U.S. AMMRC monograph MS-70-3, Watertown, MA., 1970.

3. P.G. Tracy, "Elastic analysis of radial cracks emanating from the outer and inner surfaces of a circular ring", J. Engng. Fracture Mechanics, Vol. 11, pp. 291-300, 1979.

4. P.G. Tracy, "Analysis of a radial crack in a circular ring segment", J. Engineering Fracture Mechanics, Vol. 7, pp. 253-260, 1975.

5. A.F. Emery and C.M. Segedin, "The evaluation of stress intensity factors for cracks subjected to tension, torsion, and flexure by an efficient numerical technique", J. Basic Engng. Trans. ASME, Vol. 94, pp. 387-393, 1972.

6. R. Labbens, A. Pellissier-Tanon, and J. Heliot, "Practical method for calculating stress intensity factors through weight functions" in Mechanics of Crack Growth, ASTM, STP 590, pp. 368-384, 1976.

7. C.B. Buchalet and W.H. Bamford, "Stress intensity factor solutions for continuous surface flaws in reactor pressure vessels", in Mechanics of Crack Growth, ASTM, STP 590, pp. 385-402, 1976.

8. J. Dundurs, "Elastic interaction of dislocations with inhomogeneities", in Mathematical Theory of Dislocations, ed. T. Mura, pp. 70-115, 1969.

9. R.W. Little, Elasticity, Prentice Hall, 1973.

10. F. Erdogan, "Mixed boundary value problems in mechanics", Mechanics Today, S. Nemat-Nasser, ed., Vol. 4, pp. 1-86, Pergammon Press, 1978.

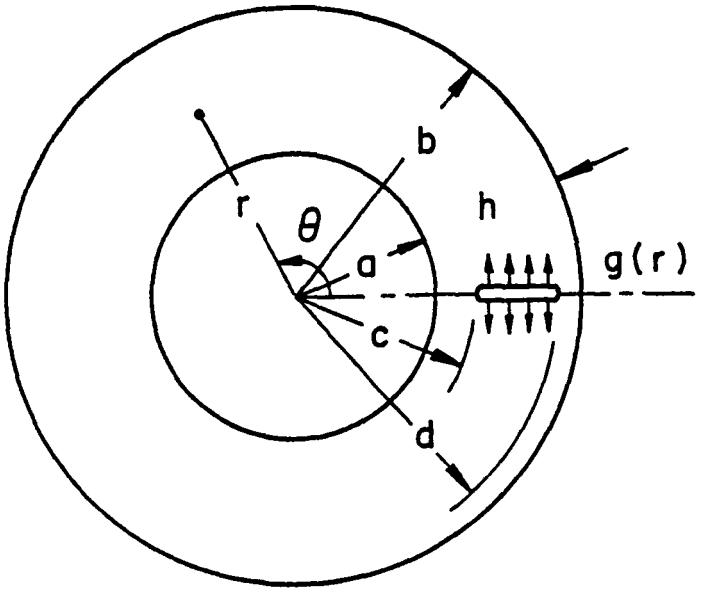

(a)

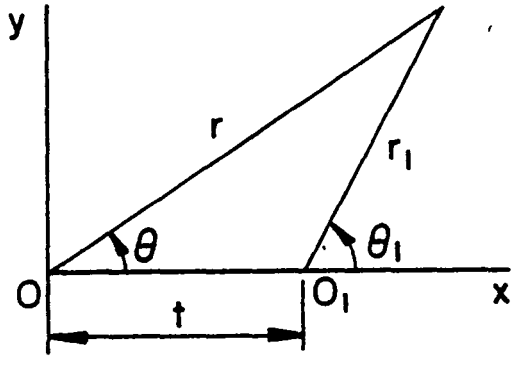

(b)

Figure 1. The geometry of the problem.

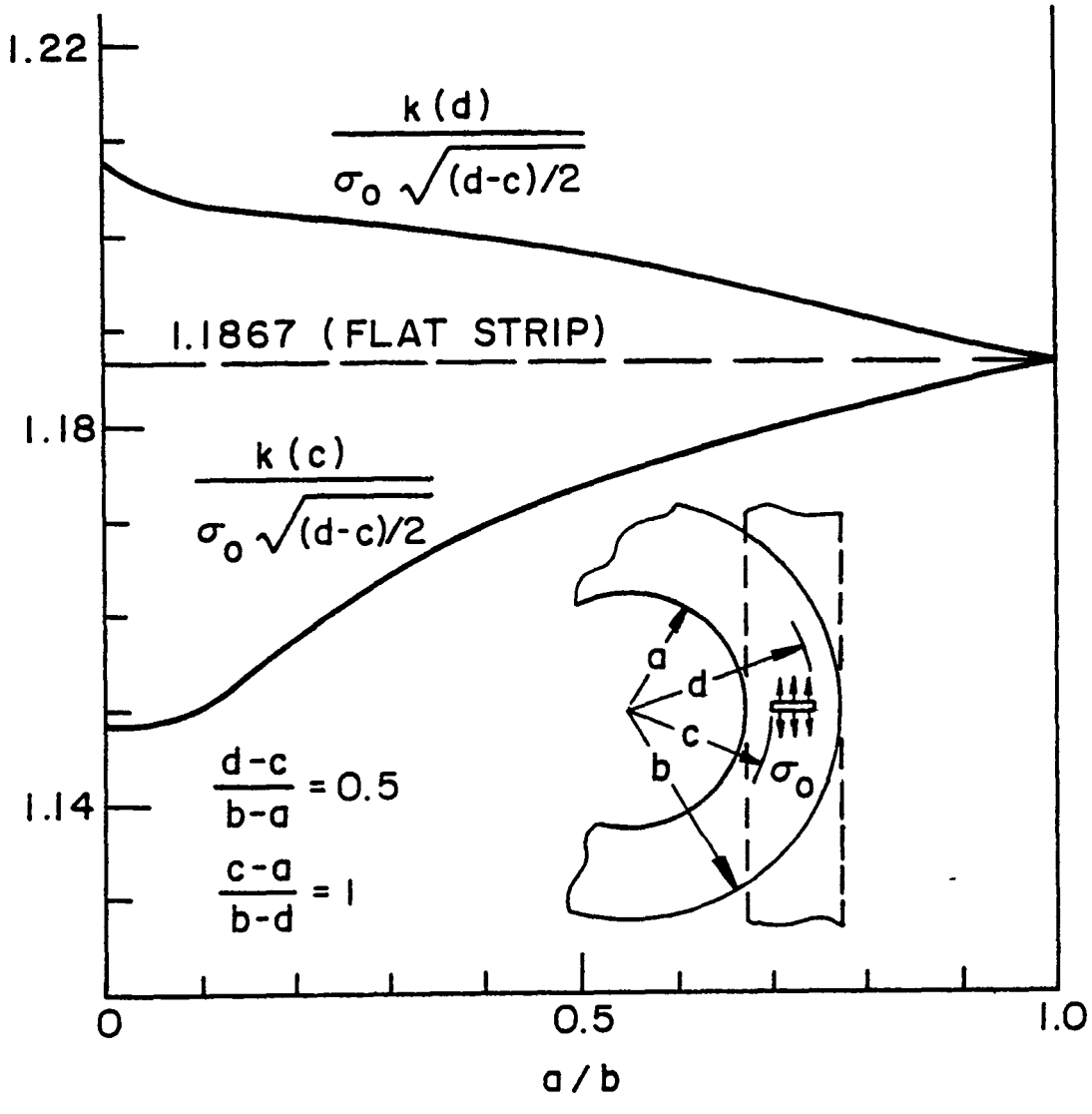

Figure 2. Stress intensity factors for an embedded crack in a hollow cylinder or a disk loaded by a uniform crack surface pressure $\sigma_{\theta\theta}(r,0) = -\sigma_0$, $c<r<d$.

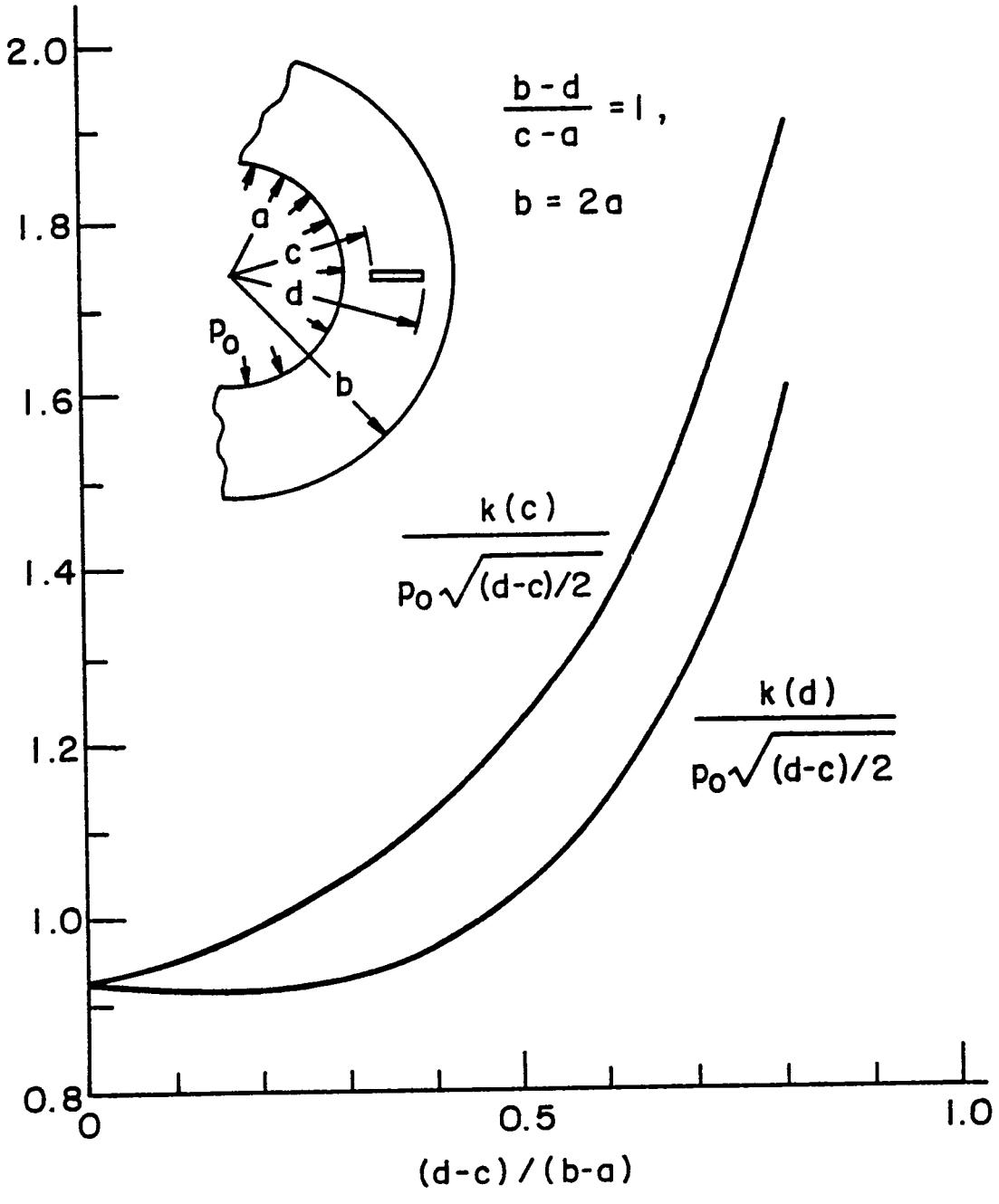

Figure 3. Stress intensity factors for an embedded crack in a hollow cylinder or a disk under internal pressure $\sigma_{rr}(a,\theta) = -p_o$.

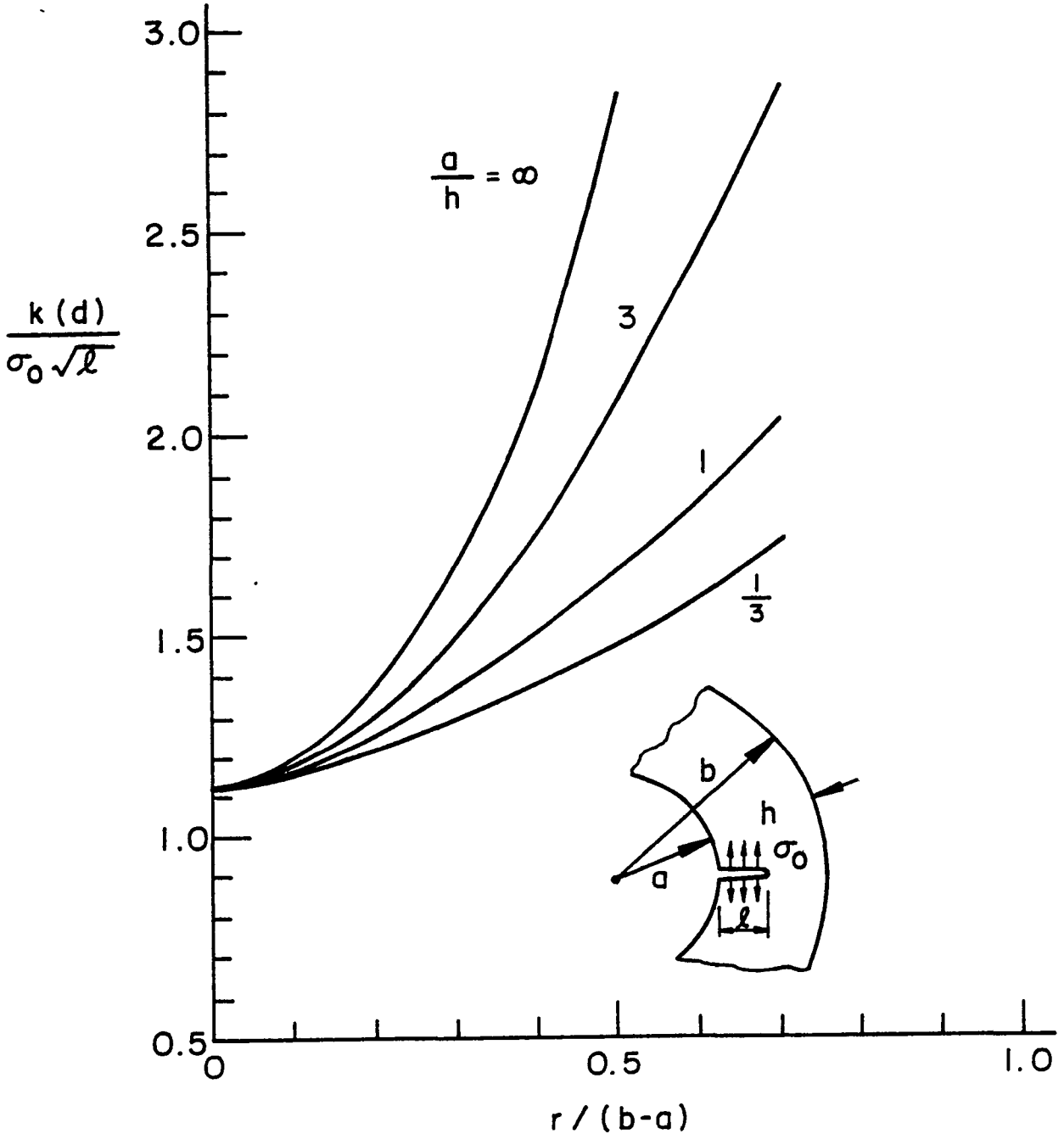

Figure 4. The stress intensity factor for an internal edge crack in a hollow cylinder or a disk loaded by a uniform crack surface pressure $\sigma_{\theta\theta}(r,0) = -\sigma_o$, ℓ=d-a.

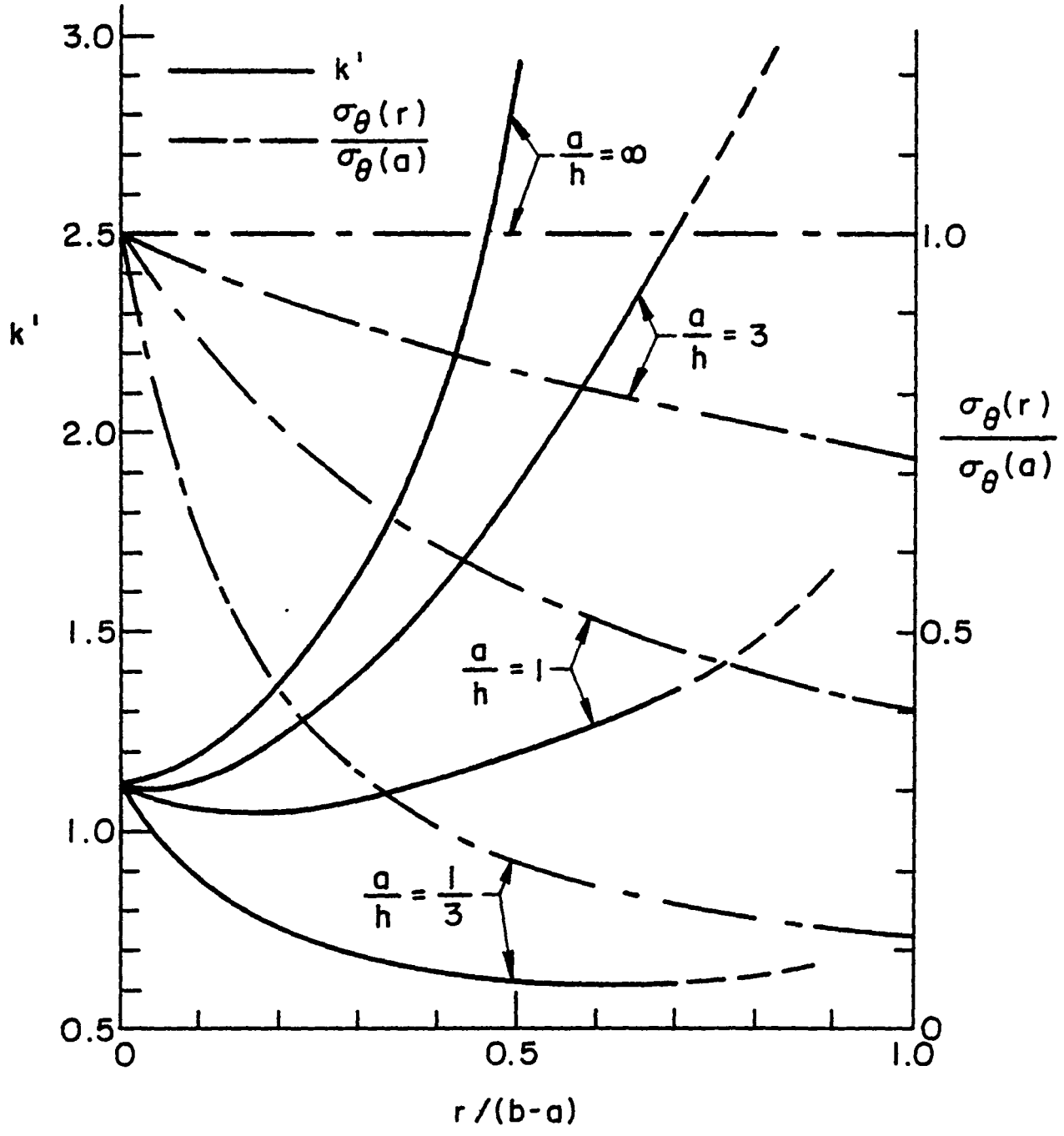

Figure 5. The stress intensity factor ratio $k' = k(d)/[\sigma_{\theta\theta}(a,0)\sqrt{d-a}]$ and the normalized hoop stress $\sigma_{\theta\theta}(r)/\sigma_{\theta\theta}(a,0)$ in a hollow cylinder or a disk containing an internal edge crack and subjected to the internal pressure $\sigma_{rr}(a,\theta) = -p_0$; $\sigma_{\theta\theta}(a,0) = p_0(b^2+a^2)/(b^2-a^2)$ (The effect of the pressure p_0 on the crack surfaces are not included).

End of Document